Asian Journal of Chemistry; Vol. 26, No. 3 (2014), 714-718

ASIAN JOURNAL OF CHEMISTRY

http://dx.doi.org/10.14233/ajchem.2014.15491

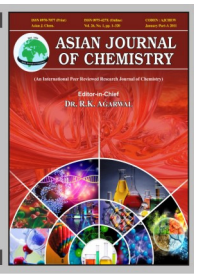

Characterization of Spinel-type $LiAl_xMn_{2-x}O_4$ Prepared by Liquid-phase Combustion Synthesis

MIMI CHEN[1,2], XIANYAN ZHOU[1,2], CHANGWEI SU[1,2], MINGWU XIANG[1,2] and JUNMING GUO[1,2,*]

[1]Key Laboratory of Chemistry in Ethnic Medicinal Resources, State Ethnic Affairs Commission & Ministry of Education, Yunnan University of Nationalities, Kunming 650500, P.R. China
[2]School of Chemistry and Biotechnology, Yunnan University of Nationalities, Kunming 650500, P.R. China

*Corresponding author: E-mail: guojunming@tsinghua.org.cn

Received: 16 March 2013; *Accepted*: 12 September 2013; *Published online*: 30 January 2014; AJC-14620

$LiAl_xMn_{2-x}O_4$ with submicron-sized particles were synthesized by liquid-phase combustion synthesis method at 500 °C for 3 h. $LiNO_3$, $Li(OAc)_2{\cdot}2H_2O$, $Mn(NO_3)_2$, $Mn(OAc)_2{\cdot}4H_2O$ and $Al(NO_3)_3{\cdot}9H_2O$ were used as raw materials. The X-ray diffraction pattern of products suggested they included a less impurity of Mn_3O_4 and a main $LiMn_2O_4$ phase with a spinel structure except that $LiAl_{0.08}Mn_{1.92}O_4$ had a single phase of $LiMn_2O_4$. Cycle performance revealed that Al doping samples ($x \leq 0.10$) possessed higher initial discharge capacity. Moreover, capacity fading could be suppressed by doped-Al. Especially, $LiAl_{0.08}Mn_{1.92}O_4$ exhibited the highest value of 116.4 mAh/g and the highest retention of 82.3 % after 40 cycles. The data of cycle voltammetry and electrochemical impedance spectrum (EIS) indicated that polarization and charge transfer impedances (R_{ct}) of $LiAl_xMn_{2-x}O_4$ were reduced by doped-Al, suggesting better reversiblities of Li^+ insertion/extraction.

Keywords: Lithium ion cathode material, $LiAl_xMn_{2-x}O_4$, Al-doped, Spinel $LiMn_2O_4$, Liquid-phase combustion synthesis.

INTRODUCTION

Lithium manganese oxide (Li-Mn-O) is regarded as a promising commercial cathode material because of its lower price, extensive availability in natural sources and environment friendly[1-5]. However, its fast capacity fading with cycling number especially at elevated temperature[6,7] is the biggest obstacle for its commercial application. Up to now, doping[8,9] is considered to be an effective path to improve the capacity retention of spinel $LiMn_2O_4$, so various metals ions were doped at the Mn-site[10-15].

As well known, the discharge capacity and cycle performance of $LiMn_2O_4$ were greatly determined by its synthesis methods and experimental conditions. There are several traditional methods to prepare this material, such as solid-state method which needs high temperature[16], microwave synthesis method[17], sol-gel method[18], coprecipitation[19], Pechini[20] and combustion method[21], *etc*. Recently, an improved combustion method called liquid-phase combustion synthesis (LCS), has been proposed by our group[22,23]. This method uses flammable and oxidative salts as raw materials, at the same time adding oxidant into, then calcineing at a low temperature to obtain very fluffy products. This method gives $LiMn_2O_4$ with a nanoparticle or submicro-particle size, uniform composition and high capacity. In a word, this possesses following merits: less energy consumption, less impurity in the products and environment friendly.

To inhibit capacity fading, Al was selected to be doped into $LiMn_2O_4$ in this paper. To the best of our knowledge, no Al-doped cathode materials with this method have been reported. In this study, the spinel $LiAl_xMn_{2-x}O_4$ was synthesized by liquid-phase combustion synthesis (LCS) method and the effect of several synthetic parameters were discussed. Fourier transform infrared (FTIR), X-ray diffraction (XRD), scanning electron microscopy (SEM), cyclic voltammogram cycle voltammetry, electrochemical impedance spectroscopy (EIS) and charge-discharge tests were used to characterize the obtained spinel $LiAl_xMn_{2-x}O_4$. The optimal Al-dopant mount is determined.

EXPERIMENTAL

$LiAl_xMn_{2-x}O_4$ ($x = 0$, 0.02, 0.05, 0.08, 0.1 and 0.2) were prepared by LCS method. $LiNO_3$ (AR, Shanghai Chemical Reagent Co., Ltd. Hanson, China), $Li(OAc)_2{\cdot}2H_2O$ (AR, Shanghai Fengshun Fine Chemical Reagent Co., Ltd., China), $Mn(NO_3)_2$ (AR, Tianjin Fengchuan Chemical Reagent Science and Technology Co., Ltd. , China), $Mn(OAc)_2{\cdot}4H_2O$ (AR, National Pharmaceutical Group Chemical Reagent Co., Ltd. , China) and $Al(NO_3)_3{\cdot}9H_2O$ (AR, Shanghai Sanpu Chemical Reagent Co., Ltd. , China) with molar ratio of Li:Mn:Al = 1:2-x:x, NO_3^-:OAc^- = 1 were weighed accurately into 300 mL crucibles, heated in a drum wind drying oven for 15 min and then removed into a muffle furnace keeping temperature 500 °C for 3 h. Lastly, the target powdery products obtained were

cooled off to room temperature and preserved into several plastic bags.

Characterization: The powders were characterized using X-ray diffraction (XRD, D/max-rB, Japan) with Cu-K_α radiation in steps of 0.02° over the range $10° \le 2\theta \le 70°$ for every sample. Tube voltage and current was 40 kV and 30 mA, respectively. Their morphologies were analyzed by scanning electron microscopy (SEM, FEI, Quanta 200, Japan) at a magnification of 60000. A Fourier transform infrared (FTIR) spectroscope (Thermo Fisher SCIENTIFIC Nicolet IS10, USA) was used to detect the change of Mn-O band, with a pellet containing a mixture of KBr and the prepared active material in the region of 800-400 cm^{-1}.

Electrochemical properties: The electrochemical performances were evaluated by means of a standard CR2025 coin cell composed of the cathode, lithium anode, a Celgard 2320 film separator, 1 M $LiPF_6$ in EC/DMC (1:1 in volume) as electrolyte. Products (80 wt %) were mixed with carbon black (10 wt %) and polyvinylidene fluoride binder (10 wt %) in a N-methyl-pyrrolidone solvent and then the mixture was uniformly pasted onto an aluminum foil, dried in an oven at 80 °C for 4 h. Subsequently the Al foil cohered $LiAl_xMn_{2-x}O_4$ was punched into numerous circular disks with 16 mm diameter. As such the cathodes were prepared. All cells were assembled in an argon-filled glove box. The cells were aged for 24 h before they were cycled in the voltage 3.2-4.35 V with 0.2 C current density at room temperature. Electrochemical charge-discharge experiments were performed at Land electric test system CT2001A (Wuhan Jinnuo Electronic Co., Ltd). Cyclic Voltammogram and electrochemical impedence spectroscopy (EIS) experiments were operated using Model CHI604D Electrochemical Instruments (Shanghai Chenhua instrument Co., Ltd) at room temperature. The voltage range was 3.2-4.35 V after the coin cells were cycled 10 times and the frequency range was 100 kHz to 0.1 Hz and the amplitude of the perturbation signal was 10 mV.

RESULTS AND DISCUSSION

Fourier transform infrared (FTIR) analysis: The FTIR spectrograms of $LiAl_xMn_{2-x}O_4$ prepared by LCS method at 500 °C are shown in Fig. 1. The two peaks, centered at about 615 and 519 cm^{-1}, are assigned to ν(Mn-O) band associating with the asymmetric stretching modes of the MnO_6 octahedral[24] and all the peaks are broad. With increasing of Al amount, the peak of 615 cm^{-1} has little displacement, but the peak of 519 cm^{-1} shift slightly toward a higher wavenumber. Which is due to coexistent of three MnO_6 octahedral (M = Li, Mn and Al) and it is hard to distinguish the vibrational band attributed to which one clearly. This result also implied the Al substituted partly Mn in the MnO_6 octahedra[25].

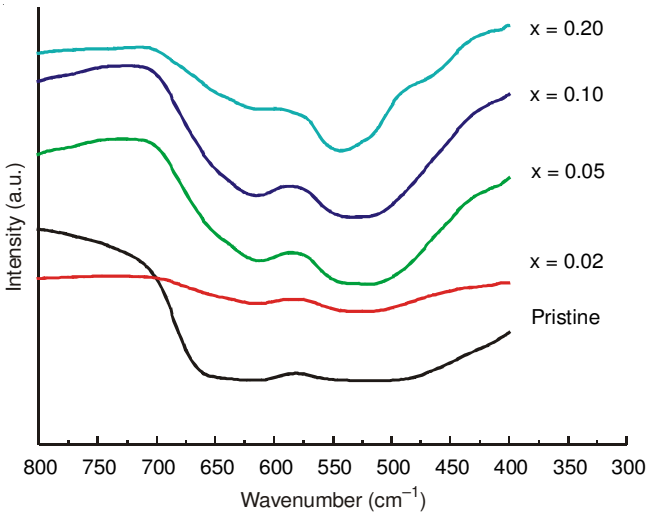

Fig. 1. FTIR of $LiAl_xMn_{2-x}O_4$ samples

X-ray diffraction analysis (XRD): XRD patterns of $LiAl_xMn_{2-x}O_4$ (x = 0.02, 0.05, 0.08, 0.1 and 0.2) are shown in Fig. 2 a. the main diffraction peaks of all the $LiAl_xMn_{2-x}O_4$ samples were ascribed to $LiMn_2O_4$ (JCPDS 35-0782) with space group Fd3m, in which the lithium ions occupy the tetrahedral sites (8a); Mn^{3+} and Mn^{4+} ions reside at the octahedral sites (16d); and O^{2-} ions are located at 32e sites[26]. This indicated that Al-doped in spinel $LiMn_2O_4$ would not change its bulk structure. The impurity of Mn_3O_4 (JCPDS 80-0382) was also observed in this Figure. Among them, $LiAl_{0.08}Mn_{1.92}O_4$ got pure spinel phase without any impurity. However, when x(Al) was up to 0.20, the diffraction peaks of impurity Mn_3O_4 became strongest. As seen in Fig. 2 (b), the lattice parameters of $LiAl_xMn_{2-x}O_4$ shrinked when doping Al. This would be caused by doped-Al substitute part of Mn resulting in shorter

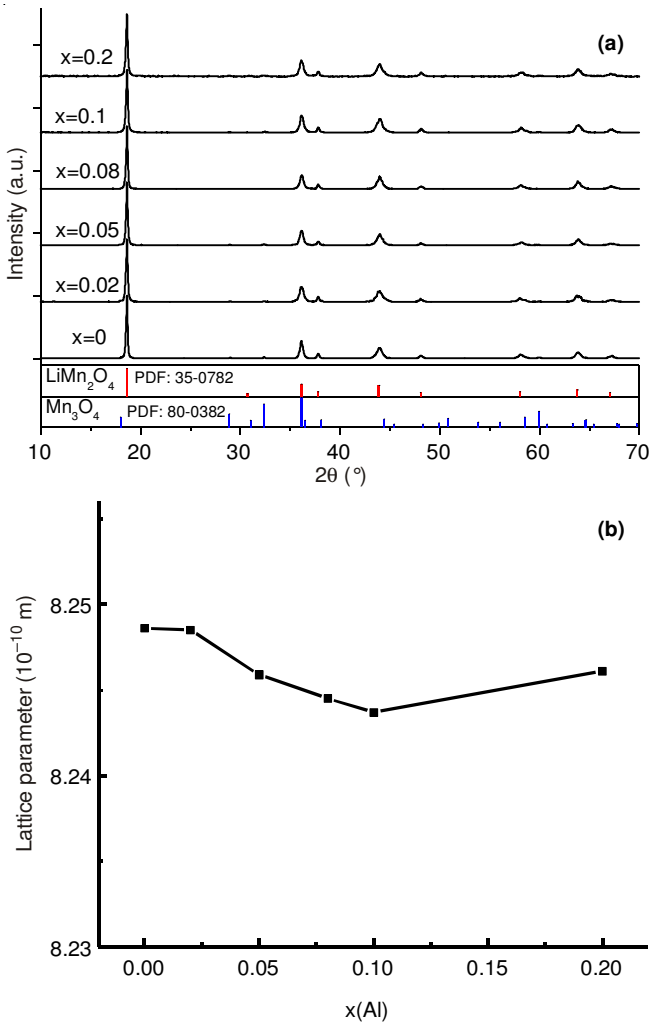

Fig. 2. (a) XRD patterns of $LiAl_xMn_{2-x}O_4$ and (b) the function between lattice parameter and the content of Al

bond length and the radius of Al^{3+} (0.530 Å) is little smaller than Mn^{3+} (0.650 Å) and the higher binding energy of Al-O than the Mn-O[27].

Scanning electron microscopy analysis: The SEM photographs of $LiAl_xMn_{2-x}O_4$ (x = 0, 0.02, 0.08 and 0.2) are showed in Fig. 3. All of the samples have agglomeration and irregular shape. However, the Al-doped samples exhibited slighter agglomeration. On these agglomerations, micro/nanoparticles can be observed. The average grain size of $LiAl_xMn_{2-x}O_4$ is 300-800 nm. According to a previous study[28], the particle size between micrometer and nanometer ranges of electrode materials is beneficial to improve cycle life, at the same time decrease slightly reaction activation.

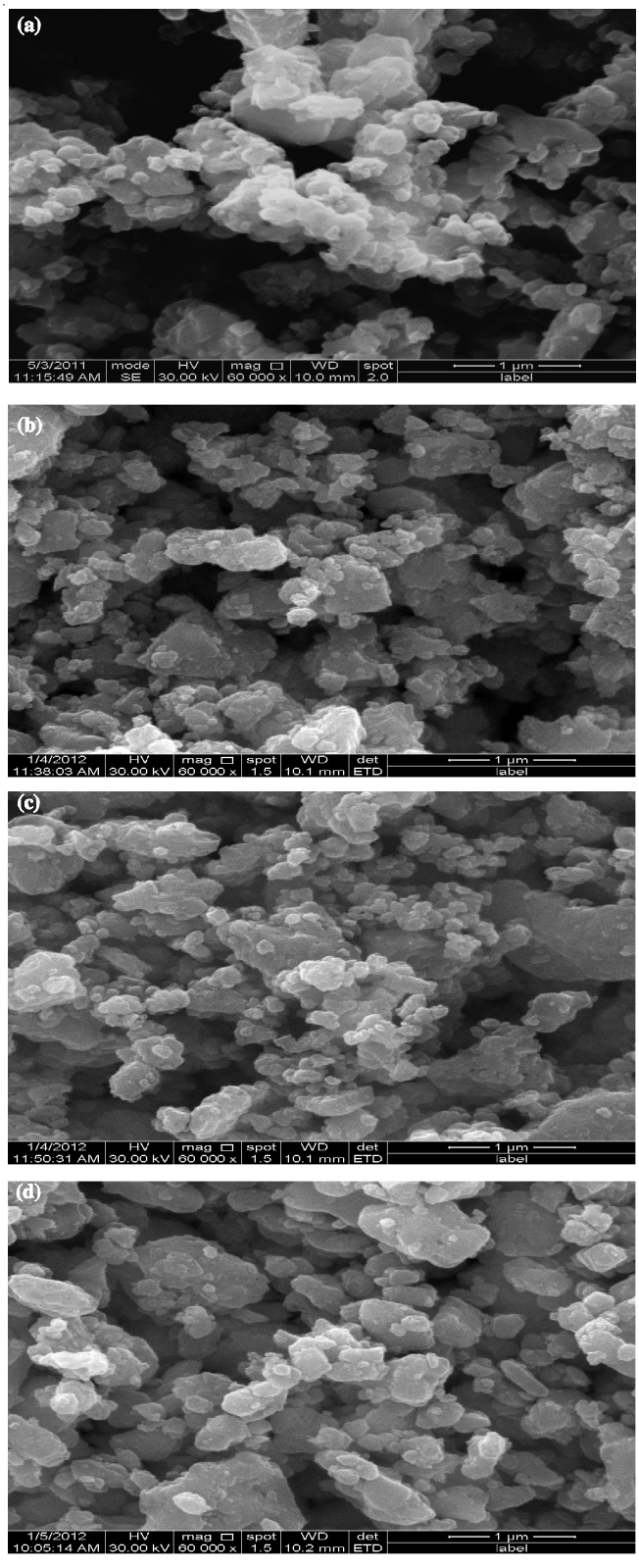

Fig. 3. SEM images of $LiAl_xMn_{2-x}O_4$ with (a) x = 0, (b) x = 0.02, (c) x = 0.08 and (d) x = 0.2

Electrochemical performance: The 10th charge-discharge curves of $LiAl_xMn_{2-x}O_4$ are shown in Fig. 4. All curves showed a distinctive two-plateau feature which is a special characteristic for spinel $LiMn_2O_4$. Kim *et al.*[29] pointed out the upper plateau of discharge curve assigned to two-phase equilibrium between MnO_2 and $Li_{0.5}Mn_2O_4$, while the lower plateau represents an equilibrium of $Li_{0.5}Mn_2O_4$ and $LiMn_2O_4$.

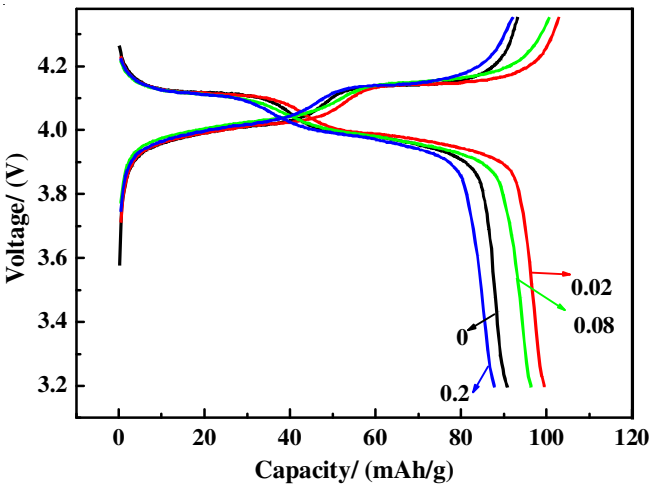

Fig. 4. The 10th charge curve for $LiAl_xMn_{2-x}O_4$ samples at 0.2 C rate

It can be seen that pristine $LiMn_2O_4$ (no Al-dopant) and $LiAl_{0.2}Mn_{1.8}O_4$ (high Al-dopant) showed the lower discharge capacity and their potential difference of charge and discharge plateaus were bigger than those of $LiAl_xMn_{2-x}O_4$ ($0.02 \le x \le 0.1$), implying strong polarization for these two cathode materials[30]. The $LiAl_xMn_{2-x}O_4$ ($0.02 \le x \le 0.10$) showed the higher discharge capacity and their potential differences of charge and discharge plateaus were smaller than pristine $LiMn_2O_4$ (no Al-dopant) and $LiAl_{0.2}Mn_{1.8}O_4$ (high Al-dopant), indicating weak polarization for the cathode material.

The cyclic performance of $LiAl_xMn_{2-x}O_4$ samples at 0.2 C rate was investigated at room temperature. Fig. 5 shows the discharge capacity *vs.* cycle number of $LiAl_xMn_{2-x}O_4$ (x = 0.02, 0.05, 0.08, 0.1 and 0.2). It can be evidently seen that the initial discharge capacity of Al-doped ($x \le 0.10$) samples were higher than that of pristine $LiMn_2O_4$ (98.1 mAh/g). The initial discharge capacity of the $LiAl_{0.08}Mn_{1.92}O_4$ cells reached 116.4 mAh/g and for $LiAl_{0.02}Mn_{1.98}O_4$, $LiAl_{0.05}Mn_{1.95}O_4$ and $LiAl_{0.10}Mn_{1.90}O_4$ samples were 107.1, 109.1 and 108.2 mAh/g, respectively. But the high Al-doped $LiAl_{0.20}Mn_{1.80}O_4$ (98 mAh/g) was lower than pristine $LiMn_2O_4$, which is possibly due to the distortion of $LiMn_2O_4$ unit cell resulting from doped Al.

The capacity retention (%) of all samples was listed in Table-1. It can be concluded that Al can be improved this electrochemical property from 5 to 22 %. For example, pristine $LiMnO_4$ reduced to 70.3 % after 40 cycles, while $LiAl_{0.08}Mn_{1.92}O_4$, remained 82.3 % after 40 cycles.

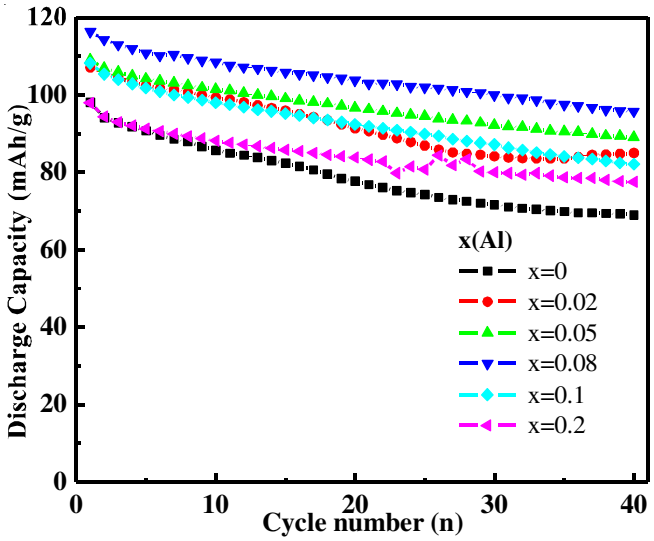

Fig. 5. Cycle performance of $LiAl_xMn_{2-x}O_4$ samples at 0.2 C rate

Cyclic voltammogram analysis: Typical 10th cyclic voltammograms of $LiAl_xMn_{2-x}O_4$ at a scan rate of 0.2 mV/s are showed in Fig. 6. It can be seen that two pairs of clearly separated peaks, which represent two redox reactions for $LiMn_2O_4$, are located at around 3.85, 4.06 and 4.1, 4.25 V. These results correspond to the typical two-step reversible insertion/deinsertion processes of lithium ion. In the spinel $LiMn_2O_4$, the oxygen ions form a cubic close-packed array, tetrahedral (8a) sites[31].

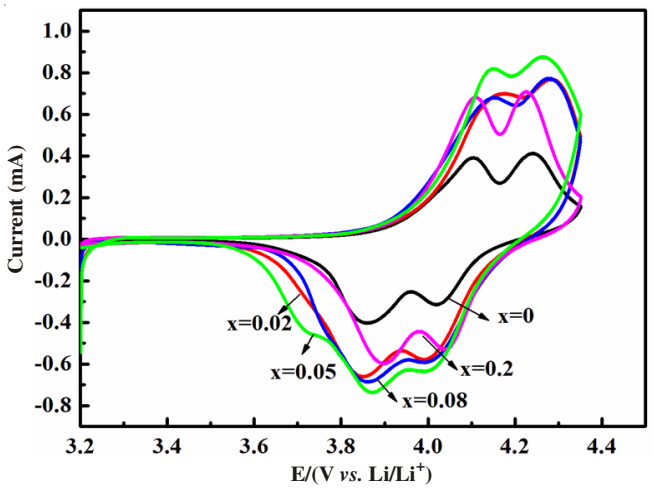

Fig. 6. Cyclic voltammograms of $LiAl_xMn_{2-x}O_4$ samples at the scanning rate of 0.2 mV/s

The current peaks of Al-doped samples were also significantly higher than that of pristine $LiMn_2O_4$, meaning that they had higher electrochemical activity[32]. The electrochemical activity could be affected slightly by Al content in samples, (Fig. 6) that the current peak firstly increased and then reduced with the increase of Al content and the $LiAl_{0.05}Mn_{1.95}O_4$ gave the highest current peak. The onset of cathodic and anodic current peaks of these $LiAl_xMn_{2-x}O_4$ samples also occurred negative and positive shift, respectively. These resulted indicated doped Al could reduce electrochemical polarization of $LiMn_2O_4$. Moreover, low potential differences of the two pairs of redox reactions suggested better reversibility for the samples.

Electrochemical impedance spectroscopy (EIS) analysis: Nyquist plots of $LiAl_xMn_{2-x}O_4$ samples obtained after 10 charge-discharge cycles are shown in Fig. 7. The plot for every one consists of a high-frequency semicircle and a low-frequency linear segment. It can be seen that the semicircle diameter (charge transfer resistance, R_{ct}) firstly decreased and then increased with increasing Al content from 0 to 0.2. Lower R_{ct} means easier insertion/extraction of Li^+ in $LiAl_xMn_{2-x}O_4$. Among all samples, the R_{ct} of $LiAl_{0.08}Mn_{1.92}O_4$ reaches the minimum value, which is possibly due to its lower lattice parameter (Fig. 2).

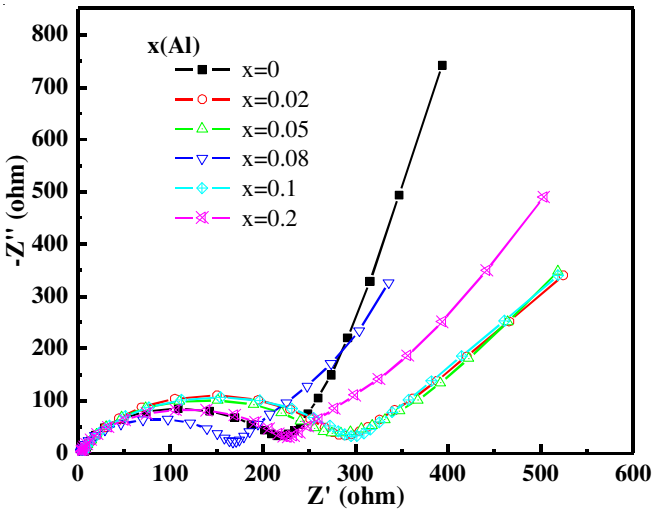

Fig. 7. Nyquist plots of electrodes of $LiAl_xMn_{2-x}O_4$ samples obtained after 10 cycles at charged state

The low-frequency lines indicated that the electrode processes are mainly controlled by diffusion. However, their slopes are all higher than $\pi/4$, implying that there are other rate-determining steps during diffusion. Comparing with pristine $LiMn_2O_4$, Al-doped samples exhibited a low slope closing to $\pi/4$. This result suggests that doped Al can suppress the other rate-determining steps.

In this paper, $LiAl_xMn_{2-x}O_4$ ($x \leq 0.20$) submicron-sized particles were fabricated by liquid-phase combustion synthesis method at 500 °C for 3 h. The obtained powders were composed of a main $LiMn_2O_4$ spinel phase and a little impurity Mn_3O_4

TABLE-1
THE CAPACITY RETENTION RATE (%) OF $LiAl_xMn_{2-x}O_4$ SAMPLES AT 0.2 C RATE

x	0	0.02	0.05	0.08	0.1	0.2
Initial discharge capacity (mAh/g)	98.1	107.1	109.1	116.4	108.2	98
Discharge capacity after 40th cycle (mAh/g)	69	85.1	89.1	95.8	82.1	77.5
The capacity retention rate (%)	70.3	79.5	81.7	82.3	75.9	79.1

phase except that $LiAl_{0.08}Mn_{1.92}O_4$ had a single phase of $LiMn_2O_4$. The cycle performance revealed that Al doping ($x \leq 0.10$) samples exhibited higher initial discharge capacity of which $LiAl_{0.08}Mn_{1.92}O_4$ was up to the highest value of 116.4 mAh/g and the highest retention of 82.3 % after 40 cycles. The electrochemical tests (Change-discharge, CV and EIS) revealed that the $LiAl_{0.08}Mn_{1.92}O_4$ synthesized has the best electrochemical performance.

ACKNOWLEDGEMENTS

This work was supported by the National Natural Science Fundation of China (51062018, 51262031), The Natural Science Fundation of Yunnan (2010FXW004), Program for Innovative Research Team (in Science and Technology) in University of Yunnan Province (2010UY08, 2011UY09), Yunnan Provincial Innovation Team (2011HC008) and Program for Innovative Research for Graduate Students in Yunnan University of Nationalities (2012YCX16).

REFERENCES

1. J.M. Tarascon and M. Armand, *Nature,* **414**, 359 (2001).
2. T. Tanaka, K. Ohta and N. Arai, *J. Power Sources*, **97-98**, 2 (2001).
3. R. Hamlen, G. Au, M. Brundage, M. Hendricks, E. Plichta, S. Slane and J. Barbarello, *J. Power Sources*, **97-98**, 22 (2002).
4. R.A. Marsh, S. Vukson, S. Surampudi, B.V. Ratnakumar, M.C. Smart, M. Manzo and P.J. Dalton, *J. Power Sources*, **97-98**, 25 (2001).
5. B. Deng, H. Nakamura and M. Yoshio, *J. Power Sources*, **141**, 116 (2005).
6. Y.Y. Xia, T. Sakai, T. Fujieda, X.Q. Yang, X. Sun, Z.F. Ma, J. McBreen and M. Yoshio, *J. Electrochem. Soc*., **148**, A723 (2001)
7. K.Y. Chung, H.S. Lee, W.S. Yoon, J. McBreen and X.Q. Yang, *J. Electrochem. Soc*., **153**, A774 (2006).
8. Y.P. Wu, E. Rahm and R. Holze, *Electrochim. Acta*, **47**, 3491 (2002).
9. G. Amatucci, A. Du Pasquier, A. Blyr, T. Zheng and J.-M. Tarascon, *Electrochim. Acta*, **45**, 255 (1999).
10. J.H. Lee, J.K. Hong, D.H. Jang, Y.K. Sun and S.M. Oh, *J. Power Sources*, **89**, 7 (2000).
11. M. Yoshio, Y. Xia, N. Kumada and S. Ma, *J. Power Sources*, **101**, 79 (2001).
12. S. Komaba, K. Oikawa, S.T. Myung, N. Kumagai and T. Kamiyama, *Solid State Ionics*, **149**, 47 (2002).
13. Z.D. Peng, Q.L. Jiang, K. Du, W.G. Wang, G.R. Hu and Y.X. Liu, *J. Alloys Comp*., **493**, 640 (2010).
14. Y.D. Huang, J. Li and D.Z. Jia, *J. Colloid Interf. Sci*., **286**, 263 (2005).
15. W. Lu, I. Belharouak, S.H. Park, Y.K. Sun and K. Amine, *Electrochim. Acta*, **52**, 5837 (2007).
16. J.M. Tarascon, E. Wang, F.K. Shokoohi, W.R. Mckinnon and S. Colson, *J. Electrochem. Soc*., **138**, 2859 (1991).
17. M. Nakayama, K. Watanabe, H. Ikuta, Y. Uchimoto and M. Wakihara, *Solid State Ionics*, **164**, 35 (2003).
18. R. Dziembaj and M. Molenda, *J. Power Sources*, **119**, 121 (2003).
19. T.H. Cho, M. Makidera, H. Nakamura and M. Yoshio, *Electrochemistry*, **71**, 1087 (2003).
20. W. Liu, G.C. Farrington, F. Chaput and B. Dunn, *J. Electrochem Soc*., **143**, 879 (1996).
21. W.S. Yang, G. Zhang, J.Y. Xie, L.L. Yang and Q.G. Liu, *J. Power Sources*, **81-82**, 412 (1999).
22. Y. Xia, M. Huang, J.M. Guo and Y.J. Zhang, *Appl. Mech. Mater*., **80-81**, 332 (2011).
23. M. Huang, Y. Xia, J.M. Guo and Y.J. Zhang, *Appl. Mech. Mater*., **80-81**, 153 (2011).
24. P. Kalyani and N. Muniyandi, *J. Power Sources*, **111**, 232 (2000).
25. Y. Makimura and T. Ohzuku, *J. Power Sources*, **119**, 156 (2003).
26. Y.P. Fu, Y.H. Su and C.H. Liu, *Solid State Ionics*, **166**, 137 (2004).
27. B.H. Freitas, F.A. Amaral, N. Bocchi and M.F.S. Teixeira, *Electrochim. Acta*, **55**, 5659 (2010).
28. N.N. Sinha and N. Munichandraiah, *J. Solid State Electrochem*., **12**, 1619 (2008).
29. B.H. Kim, Y.K. Choi and Y.H. Choa, *Solid State Ionics*, **158**, 281 (2003).
30. Z.D. Peng, Q.L. Jiang, K. Du, W.G. Wang, G.R. Hu and Y.X. Liu, *J. Alloys Comp*., **493**, 640 (2010).
31. W.J. Zhou, S.J. Bao, Y.Y. Liang, B.L. He and H.L. Li, *J. Solid State Electrochem*., **10**, 277 (2006).
32. Y.D. Huang, R.R. Jiang, S.J. Bao, Y.L. Cao and D.Z. Jia, *Nanoscale Res. Lett*., **4**, 353 (2009).